

Diffusion abnormalities of the uncinate fasciculus in Alzheimer's disease: diffusion tensor tract-specific analysis using a new method to measure the core of the tract

Hasina Yasmin · Yasuhiro Nakata · Shigeki Aoki · Osamu Abe · Noriko Sato · Kiyotaka Nemoto · Kunimasa Arima · Nobuo Furuta · Masatake Uno · Shigeo Hirai · Yoshitaka Masutani · Kuni Ohtomo

Received: 15 July 2007 / Accepted: 7 December 2007 / Published online: 2 February 2008
© Springer-Verlag 2007

Abstract

Introduction Our aim was to determine diffusion abnormalities in the uncinate fasciculus (UF) in Alzheimer's disease (AD) by diffusion tensor tractography (DTT) using a new method for measuring the core of the tract.

Methods We studied 19 patients with AD and 19 age-matched control subjects who underwent MRI using diffusion tensor imaging (DTI). DTT of the UF was generated. The mean diffusivity (MD) and fractional anisotropy (FA) of the core of the tract were measured after voxelized tract shape processing. Student's *t*-test was used to compare results between patients with AD and controls. Intraobserver correlation tests were also performed.

Results FA was significantly lower ($P < 0.0001$) in the UF of patients with AD than of controls. There was no

significant difference in MD along the UF between the two groups. Intraobserver reliability (intraclass correlation coefficient) for the first and second measurement was $r > 0.93$ for measured FA and $r > 0.92$ for measured MD.

Conclusion Our results suggest that FA reflects progression of AD-related histopathological changes in the UF of the white matter and may represent a useful biological index in monitoring AD. Diffusion tensor tract-specific analysis with voxelized tract shape processing to measure the core of the tract may be a sensitive tool for evaluation of diffusion abnormalities of white matter tracts in AD.

Keywords Alzheimer's disease · Uncinate fasciculus · Diffusion tensor imaging · Diffusion tensor tractography · Tract-specific analysis

H. Yasmin · Y. Nakata · S. Aoki (✉) · O. Abe · Y. Masutani · K. Ohtomo
Department of Radiology, University of Tokyo,
7-3-1 Hongo, Bunkyo-ku,
Tokyo 113-8655, Japan
e-mail: saoki-tky@umin.ac.jp

N. Sato
Department of Radiology, National Center Hospital for Mental,
Nervous and Muscular Disorders,
National Center of Neurology and Psychiatry,
4-1-1 Ogawahigashi, Kodaira,
Tokyo 187-8511, Japan

K. Nemoto
Department of Psychiatry, Ibaraki Prefectural Tomobe Hospital,
654 Asahimachi, Tomobe-cho, Nishiibaraki-gun,
Ibaraki 309-1717, Japan

K. Arima · N. Furuta
Department of Psychiatry, National Center Hospital for Mental,
Nervous and Muscular Disorders,
National Center of Neurology and Psychiatry,
4-1-1 Ogawahigashi, Kodaira,
Tokyo 187-8511, Japan

M. Uno
Department of Psychiatry, Yoshioka Rehabilitation Clinic,
4-2-8 Shimo-renjaku, Mitaka,
Tokyo 181-0013, Japan

S. Hirai
Department of Psychiatry, Iruma Hirai Clinic,
1-2-21 Toyooka, Iruma,
Saitama 358-0003, Japan

Introduction

Alzheimer's disease (AD) is a neurodegenerative disease characterized by progressive cognitive deterioration together with declining activities of daily living and neuropsychiatric symptoms or behavioral changes. It is the most common type of dementia. Neuroimaging research has suggested that magnetic resonance imaging (MRI) might serve as a more sensitive and consistent measure of disease progression than the neuropsychological and cognitive assessments that are typically used in present-day research. Among the pathological changes in AD, several white matter (WM) abnormalities such as rarefaction, loss of axons and oligodendrocytes, and reactive astrogliosis have been observed [1]. In line with these observations, diffusion tensor magnetic resonance imaging (DTI) studies [2–6] have also shown microscopic WM changes in patients with AD that are not detected by conventional MRI; however, the precise topography and extent of these WM changes remain a topic of debate.

DTI is a noninvasive technique that enables the user to visualize in three dimensions and quantify the organization and integrity of white matter fiber tracts in the human brain in vivo [7, 8]. Diffusion tensor-derived parameters such as fractional anisotropy (FA) and mean diffusivity (MD) can thus describe the microarchitectural characteristics of local brain tissue, and mapping of these parameters can be used to depict pathological changes in the cerebral white matter. Several recent reports have shown that mapping of diffusion parameters is potentially useful in diagnosing AD [2, 3, 5, 9–18]. DTI can characterize the properties of water diffusion in the brain by providing three types of information: the extent (apparent diffusion constant, ADC) and directionality (anisotropy) of diffusion, and its predominant orientation [7, 19]. ADC and anisotropy are believed to be related predominantly to the integrity of axonal tracts [20, 21], and depict contrast that is different from that in conventional T1- and T2-weighted images [19]. Tract-specific analysis (TSA) by DTI is one of the most promising image-processing techniques that enables visualization of fiber pathways in the brain as well as quantitative analysis of specific fiber bundles [22–24]. There is considerable interest in DTI-based TSA because it may enable an improved understanding of the disruptions in connections between brain regions, which have otherwise yet to be quantitatively evaluated.

Previous studies indicate that AD is associated with changes in the white matter of the frontal and temporal lobes [10, 17]. The uncinate fasciculus (UF) is a white matter tract that connects the anterior part of the temporal lobe with the orbital and polar frontal cortex; it is believed to play a role in emotion, decision-making and episodic memory, and in the pathophysiology of AD [22, 25–27].

Several experimental studies have shown that the UF is a monosynaptic corticocortical route of interaction between the temporal and frontal lobes. Review of many experimental studies supports the role of the UF as one of several connections whose disruption results in severe memory impairment [26, 28]. The disruption in connectivity between the temporal and frontal lobes via the UF is postulated as a possible cause of posttraumatic retrograde amnesia [26, 29].

The aim of the present study was to perform a tract-specific assessment of diffusion properties of the UF in patients with AD in comparison with normal controls. Until now it has been difficult to evaluate only a specific tract of interest. No method has successfully minimized partial volume effects in TSA, and a reconstructed fiber tract is always associated with incidental artifactual lines. We propose a new technique for measuring the core of the tract in TSA using the erosion method, which eliminates incidental artifactual lines and partial volume effects.

Materials and methods

Participants

From a consecutive series of 55 subjects enrolled in a prospective study of patients with AD and a chief complaint of dementia, we retrospectively selected 19 patients (11 female and 8 male; mean age 71.1 ± 8.1 years, age range 55–81 years) who were diagnosed as probably having AD according to the criteria of the National Institute of Neurological and Communicative Disease and Stroke and the Alzheimer's Disease and Related Disorders Association [30]. The patients had attended the Department of Radiology at the National Center Hospital for Mental, Nervous, and Muscular Disorders, National Center of Neurology and Psychiatry, Tokyo, Japan, from March to July 2005. Three patients did not meet the criteria. Six patients who presented with major systemic, psychiatric or other neurological illness, or head trauma were excluded. Excluded from the study were 16 patients who presented with significant cerebrovascular diseases (cortical infarction, multiple lacunar lesions, leukoariosis or other lesions above Fazekas grade 1 [31]) on T2-weighted or FLAIR images, and 11 patients with an unsatisfactory DTI study due to artifacts originating from patient motion or metallic dental prostheses. Also recruited were 19 age-matched healthy controls (12 female and 7 male; mean age 69.0 ± 5.3 years, age range 62–80 years) who did not have any neurological or psychiatric conditions, had no cognitive complaints, had a normal neurological examination, and were not taking any antipsychotic medications.

We obtained local ethics committee approval and written informed consent from all patients and healthy controls before initiation of the study.

Cognitive screening

To obtain an overall assessment of cognitive function, each subject was administered the Mini Mental State Examination (MMSE) by a trained neuropsychologist. The mean MMSE score was 21.6 ± 5.3 (range 9–29) for patients with AD and 28.5 ± 1.4 (range 25–30) for control subjects.

MRI acquisition

All scans were performed using a 1.0-T MRI system (Magnetom Harmony; Siemens, Erlangen, Germany) with a standard head coil. We obtained regular structural images prior to DTI acquisition that included T1-weighted spin echo images (TR 624 ms, TE 15 ms, matrix size 512×416 , FOV 230×230 mm, slice thickness 5 mm, intersection gap 0.4 mm, number of acquisitions 1), T2-weighted turbo-spin echo images (TR 6,580 ms, TE 89 ms, matrix size 512×432 , FOV 230×230 mm, slice thickness 5 mm, intersection gap 0.4 mm, number of acquisitions 1), and FLAIR images (TR 9,100 ms, TE 104 ms, TI 2500 ms, matrix size 512×448 , FOV 230×230 mm, slice thickness 5 mm, intersection gap 0.4 mm, number of acquisitions 1).

DTI was performed using a full tensor diffusion MRI sequence based on the spin-echo echo-planar technique (TR 8,400 ms, TE 113 ms, matrix size 128×128 , FOV 230×230 mm, slice thickness 3 mm with no gap). Images were obtained with both 12-directional diffusion encoding ($b=700$ s/mm² for each direction) and no diffusion encoding ($b=0$ s/mm²). To ensure high data reliability, a high signal-to-noise ratio was achieved by averaging images six times. A total of 40 sets of axial images were obtained covering the whole cerebrum. Scanning time for DTI was 11 min 7 s.

DTI data postprocessing

DTI data were transferred to an off-line workstation. Analysis was performed using dTV II and VOLUME-ONE 1.72 developed by Masutani et al. [32] (<http://www.ut-radiology.umin.ac.jp/people/masutani/dTV.htm>) running under Windows XP Professional (Microsoft, Redmond, WA). Interpolation along the z-axis was performed to obtain isotropic data (voxel size $1.8 \times 1.8 \times 1.8$ mm).

We created color-coded maps using 13 sets of images (12 sets of images with $b=700$ s/mm², 1 set of images with $b=0$ s/mm²). Green was assigned to anteroposterior, red to left–right, and blue to the craniocaudal direction in the axial, coronal, and sagittal slices [33]. Color-coding of the

fiber orientation enabled ready identification of major white matter tracts by comparison with previously published data on DTI of white matter association pathways [34].

Tractography of bilateral UF was performed using the two-ROI method [32, 35]. The seed ROIs were set in the anterior part of the UF in the coronal plane at the level of the anterior portion of the genu of the corpus callosum, just anterior to the anterior horn of the lateral ventricle. The target ROIs were set in the white matter in the coronal plane at the most anterior part of the temporal stem. The color-coded maps were used to place these ROIs into the UF tracts precisely and objectively. A reconstructed sagittal section of the color-coded map was used to determine reconstructed coronal sections at the level of the genu of the corpus callosum (Fig. 1a). In the coronal slices, UF tracts were displayed as green. The relatively large seed ROI, including the entirety of the uncinate tracts, was placed manually on a reconstructed coronal color map section at the level of the genu of the corpus callosum (Fig. 1b). Similarly, the relatively large target ROI, including the entirety of the UF, was placed manually on a reconstructed coronal section of the T2-weighted images at the level of the anterior temporal stem (Fig. 1c). DTT of the UF was then generated using the threshold values of line-tracking termination as $FA > 0.15$ (Fig. 1d). The dTV II software provides a track-line voxelization function that extracts the tracking line of the white matter tract to the 3-D voxels while preserving the original tensor parameters. Voxelization along the UF tract was performed (Fig. 2a); all voxels including the tracked lines were encountered. We then used a shape-processing technique based on mathematical morphology [36] to reduce the partial volume effect of the peripheral portion of the tract. This technique also eliminated small incidental artifactual lines. Theoretically, there can be holes within the tracts, because even from a dense seed, fibers can be sparse. To fill up the holes, dilation is necessary. If we had voxelized the tract without dilation, some voxels could have been missed. So first we performed the closing operation (dilation, Fig. 2b, and first erosion) then we extracted the core (Fig. 2c, second erosion). The UF is relatively thin compared to voxel size. So simple erosion often leads to total disappearance of the ROI shape due to cavities within the ROI voxels. The FA and MD values in coregistered voxels were then calculated. The approximate diameters of the tracts in various steps of the above processes were also measured.

Overall DTI data processing time was approximately 20 min per subject. Measurements were repeated 1 month after the first measurement. We also performed the DTT of the UF for every subject by the conventional method (as described by Taoka et al. [22]). By this method, in order to remove the unwanted fibers we used avoidance at the level of the middle portion of the temporal lobe in the coronal

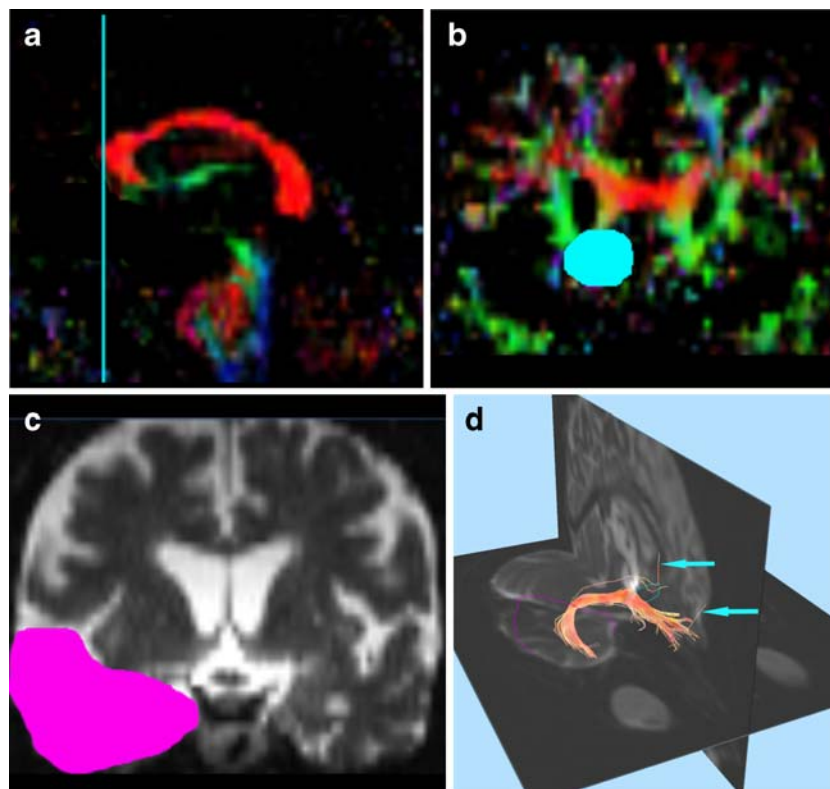


Fig. 1 Visualization of DTT of the UF in patients with AD. **a** A reconstructed sagittal section of the color-coded map was used to determine reconstructed coronal sections at the level of the genu of the corpus callosum (*sky-blue line*). **b** The relatively large seed ROI (*sky-blue area*) was placed manually on a reconstructed coronal color map section at the level of the genu of the corpus callosum. **c** The relatively

large target ROI including the entirety of the UF tracts (*purple area*) was placed manually on a reconstructed coronal T2-weighted image at the level of the anterior temporal stem. **d** DTT of the UF was generated from a seed ROI in the anterior part of the UF tracts to the target ROI in the posterior part of the UF tracts (*arrows incidental artifactual lines*)

section of the T2 weighted image. To compare our proposed new method (erosion technique) with the conventional method, we visually evaluated the voxelized tract of the UF according to the anatomical location of the fiber tract as evaluated by Kier et al. [26]. We randomly selected

ten subjects (five patients with AD, five controls). We graded the voxelized tract as grade 0 if none of the fibers was outside the anatomical location of the UF, and graded the tract as grade 1 if there were fibers outside the anatomical location of the UF.

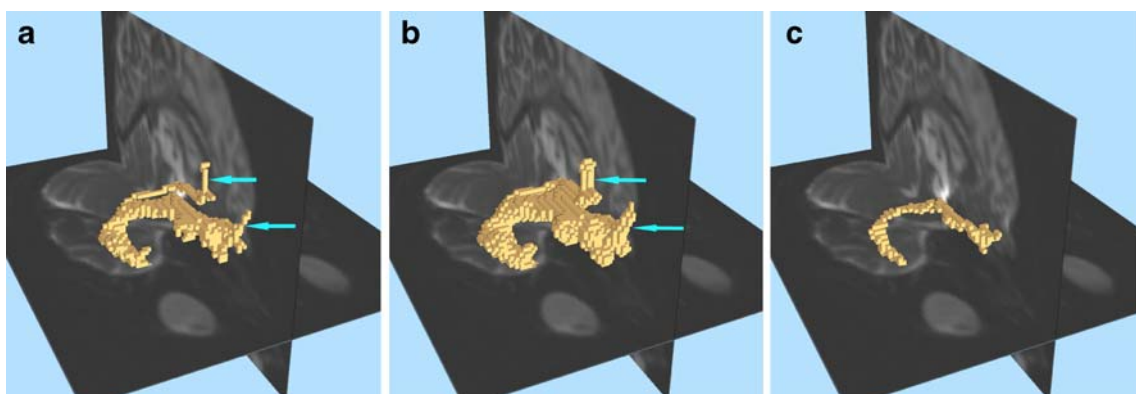


Fig. 2 Formation of the core of the UF tract. A 3-D display of the UF from the anterior upper right with background T2-weighted images in the sagittal and axial planes. **a** Voxelization along the UF tracts. **b** Voxels along the UF tracts were dilated once. **c** Removal of partial

volume effects to reveal the core of the UF tracts was achieved by erosion of the voxels. FA and MD values in coregistered voxels within the core of the UF tracts were then calculated

Statistical analysis

Statistical analyses were performed using StatView 5.0 software (SAS Institute, Cary, NC). Averaged MD and FA values of the right and left UF from the first assessment event were used. *P* values <0.05 were considered to indicate statistical significance. Intraobserver correlation tests were also performed. The data obtained from the conventional method were also analyzed using Student's *t*-test for every patient and control subject. The visual evaluation data were analyzed using Fisher's exact test.

Results

Tractographies of the UF were obtained as semicircular tracts connecting the anterior part of the temporal lobe with the orbital and polar frontal cortex in all patients with AD and controls. The mean FA values were 0.38 ± 0.018 for patients with AD and 0.42 ± 0.027 for the controls (Fig. 3). Patients with AD had significantly lower mean FA values ($P=0.0001$) than the control group. The mean MD values were $0.68 \pm 0.03 \times 10^{-3} \text{ mm}^2/\text{s}$ for patients with AD and $0.68 \pm 0.04 \times 10^{-3} \text{ mm}^2/\text{s}$ for the controls. There was no significant difference in MD. The sizes of the tracts were $12.2 \pm 2.5 \text{ mm}$ (7.2–14.4 mm) before dilation (real size of the tract), $17.1 \pm 3.9 \text{ mm}$ (9–23.4 mm) after dilation, $13.1 \pm 3.1 \text{ mm}$ (7.2–16.6 mm) after the first erosion, and $7.2 \pm 1.3 \text{ mm}$ (5.4–9 mm) after the second erosion (core of the tract). The intraobserver reliability (intraclass correlation coefficient) for the first and second measurement was $r > 0.93$ for measured FA and $r > 0.92$ for measured MD. By the conventional method, the mean FA values were 0.35 ± 0.015 for patients with AD and 0.38 ± 0.025 for controls ($P=0.0001$). All ten voxelized tracts of the UF were visually evaluated as grade 1 by the conventional method, whereas by the new method two voxelized tracts of the UF were evaluated as grade 1 and eight were evaluated as grade 0 ($P < 0.0004$, Fisher's exact test).

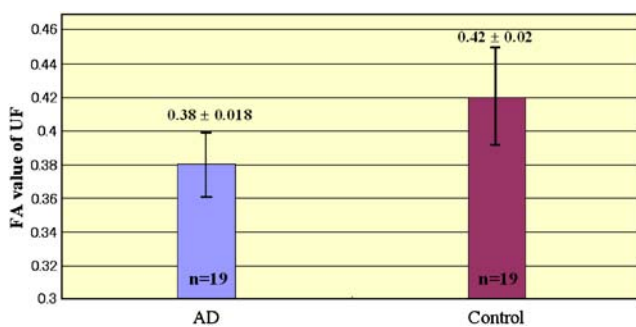


Fig. 3 FA values of the UF in patients with AD and controls

Discussion

Many studies have investigated white matter abnormalities in AD using DTI, including regions such as the hippocampus, temporal stem, posterior cingulate, and occipital and parietal white matter. A number of studies have demonstrated that FA is decreased in some patients [3, 6, 9, 13, 16–18, 22, 37]. Our results support the findings of these previous studies. In the present study, we paid particular attention to diffusion abnormalities of the UF in AD and applied a new erosion method that enabled the core of the UF to be obtained for the first time.

The UF is a hook-like fiber bundle that can be divided into temporal, insular, and frontal segments [25, 26]. The frontal segment of the UF has a fan-like shape in the frontal orbital white matter and is oriented in a horizontal plane. The fibers of the UF connect the cortical nuclei of the amygdala and the uncus with the subcallosal region. The tips of the superior, medial, and inferior temporal gyri are connected, via the UF, with the gyrus rectus and medial and lateral orbital gyri as well as the orbital segment of the inferior frontal gyrus. The UF consists of both afferent and efferent fibers to both the temporal and frontal areas [26, 38]; it has a ventral part that connects the orbital cortex with the amygdala and hippocampal gyrus, and a dorsal section that connects the temporal pole cortex with the rostral end of the middle frontal gyrus [26, 39, 40].

In the present study, visualizing DTT enabled clear identification of the UF and more precise measurement of diffusion parameters by avoiding contamination of data from adjacent structures such as CSF or callosal fibers. Our method was relatively objective because voxelization along the core of the UF was performed using DTT, compared with a simple manually drawn ROI study in which ROIs can be set anywhere. Because the white matter tracts of interest were segmented by DTT and the portion of segmented tract was evaluated selectively, our methods may be more sensitive than methods that use other anatomical landmarks. The extracted core of the tract is smaller than the real size of the tract. If we erode the shape of a tract, there is a reduction of two or three voxels depending on the direction of the tract.

To the best of our knowledge, few previous studies have used color-coded maps [7, 17], and only one previous study has used DTT [22] for DTI abnormalities in AD patients. Taoka et al. measured DTI abnormalities in the UF, inferior occipitofrontal fasciculus, and Meyer's loop using DTT in AD patients and control subjects [22]. Our study differs from that of Taoka et al. in the following regards: (a) the MMSE score of the subjects differed (21.6, range 9–29, in the present study compared with 15, range 4–22, in the study of Taoka et al.); (b) we used color maps for fiber tracking; and (c) we used an erosion technique to obtain the

core of the tract. The patient group in the study of Taoka et al. was in late AD, and there were differences in both FA and ADC of the UF; in contrast, we found differences only in FA of the UF in our study group. The results of the present study suggest that only change in FA of the UF may be significant in early-stage AD. It is unclear from their report [22] whether Taoka et al. used avoidance or not. The use of avoidance is time consuming and operator-dependent. Our new method does not require the use of any avoidance. Taoka et al. used the threshold for line tracking termination of FA values >0.18 and measured the voxels along the line of the fiber tracts. On the other hand, we used the threshold for line tracking termination of FA values >0.15 and we measured the voxels along the whole fiber tracts.

Takahashi et al. found that FA values were significantly lower in the temporal subcortical white matter, in the posterior part of the corpus callosum, and in the anterior and posterior cingulate fibers in patients with AD compared to controls [17]. Bozzali et al. found that FA values were lower in the corpus callosum as well as in the white matter of the frontal, temporal, and parietal lobes in patients with AD compared to controls [9]. In contrast, Kantarci et al. found no differences in anisotropy index between AD patients and controls [4]. We consider that this discrepancy is associated with the method of data acquisition and processing as well as the patient population.

A limitation of the present study was the relatively small number of patients. Future studies should therefore include a greater number of patients.

In conclusion, TSA using an erosion technique to segment the core of the fiber appears to be a highly sensitive and practical method for assessing white matter changes in AD. Our results suggest that FA reflects progression of AD-related histopathological changes in the UF of white matter and may represent a useful biological index in monitoring AD.

Conflict of interest statement We declare that we have no conflict of interest.

References

- Brun A, Englund E (1986) A white matter disorder in dementia of the Alzheimer type: a pathoanatomical study. *Ann Neurol* 9(3):253–262
- Bozzali M, Franceschi M, Falini A et al (2001) Quantification of tissue damage in AD using diffusion tensor and magnetization transfer MRI. *Neurology* 57(6):1135–1157
- Hanyu H, Sakurai H, Iwamoto T et al (1998) Diffusion-weighted MR imaging of the hippocampus and temporal white matter in Alzheimer's disease. *J Neurol Sci* 156(2):195–200
- Kantarci K, Jack CR Jr, Xu YC et al (2000) Regional metabolic patterns in mild cognitive impairment and Alzheimer's disease: A 1H MRS study. *Neurology* 55(2):210–217
- Rose SE, Chen F, Chalk JB et al (2000) Loss of connectivity in Alzheimer's disease: an evaluation of white matter tract integrity with colour coded MR diffusion tensor imaging. *J Neurol Neurosurg Psychiatry* 69(4):528–530
- Sandson TA, Felician O, Edelman RR et al (1999) Diffusion-weighted magnetic resonance imaging in Alzheimer's disease. *Dement Geriatr Cogn Disord* 10:166–171
- Basser PJ, Mattiello J, LeBihan D (1994) Estimation of the effective self-diffusion tensor from the NMR spin echo. *J Magn Reson B* 103:247–254
- Le Bihan D, van Zijl P (2002) From the diffusion coefficient to the diffusion tensor. *NMR Biomed* 15:431–434
- Bozzali M, Falini A, Franceschi M et al (2002) White matter damage in Alzheimer's disease assessed in vivo using diffusion tensor magnetic resonance imaging. *J Neurol Neurosurg Psychiatry* 72(6):742–746
- Choi SJ, Lim KO, Monteiro I et al (2005) Diffusion tensor imaging of frontal white matter microstructure in early Alzheimer's disease: a preliminary study. *J Geriatr Psychiatry Neurol* 18(1):12–19
- Fellgiebel A, Muller MJ, Wille P et al (2005) Color-coded diffusion-tensor-imaging of posterior cingulate fiber tracts in mild cognitive impairment. *Neurobiol Aging* 26(8):1193–1198
- Fellgiebel A, Wille P, Muller MJ et al (2004) Ultrastructural hippocampal and white matter alterations in mild cognitive impairment: a diffusion tensor imaging study. *Dement Geriatr Cogn Disord* 18(1):101–108
- Head D, Buckner RL, Shimony JS et al (2004) Differential vulnerability of anterior white matter in nondemented aging with minimal acceleration in dementia of the Alzheimer type: evidence from diffusion tensor imaging. *Cereb Cortex* 14(4):410–423
- Medina D, DeToledo-Morrell L, Urresta F (2006) White matter changes in mild cognitive impairment and AD: a diffusion tensor imaging study. *Neurobiol Aging* 27(5):663–672
- Muller MJ, Greverus D, Dellani PR et al (2005) Functional implications of hippocampal volume and diffusivity in mild cognitive impairment. *Neuroimage* 28(4):1033–1042
- Sugihara S, Kinoshita T, Matsusue E et al (2004) Usefulness of diffusion tensor imaging of white matter in Alzheimer disease and vascular dementia. *Acta Radiol* 45(6):658–663
- Takahashi S, Yonezawa H, Takahashi J et al (2002) Selective reduction of diffusion anisotropy in white matter of Alzheimer disease brains measured by 3.0 Tesla magnetic resonance imaging. *Neurosci Lett* 332(1):45–48
- Yoshiura T, Mihara F, Ogomori K et al (2002) Diffusion tensor in posterior cingulate gyrus: correlation with cognitive decline in Alzheimer's disease. *Neuroreport* 13(17):2299–2302
- Mori S, Frederiksen K, van Zijl PC et al (2002) Brain white matter anatomy of tumor patients evaluated with diffusion tensor imaging. *Ann Neurol* 51(3):377–380
- Beaulieu C, Allen PS (1994) Determinants of anisotropic water diffusion in nerves. *Magn Reson Med* 31:394–400
- Henkelman R, Stanisz G, Kim J et al (1994) Anisotropy of NMR properties of tissues. *Magn Reson Med* 32:592–601
- Taoka T, Iwasaki S, Sakamoto M et al (2006) Diffusion anisotropy and diffusivity of white matter tracts within the temporal stem in Alzheimer disease: evaluation of the "tract of interest" by diffusion tensor tractography. *AJNR Am J Neuroradiol* 27(5):1040–1045
- Aoki S, Iwata NK, Masutani Y et al (2005) Quantitative evaluation of the pyramidal tract segmented by diffusion tensor tractography: feasibility study in patients with amyotrophic lateral sclerosis. *Radiat Med* 23(3):195–199
- Kunimatsu A, Aoki S, Masutani Y et al (2004) The optimal trackability threshold of fractional anisotropy for diffusion tensor tractography of the corticospinal tract. *Magn Reson Med Sci* 3(1):11–17

25. Ebeling U, von Cramon D (1992) Topography of the uncinate fascicle and adjacent temporal fiber tracts. *Acta Neurochir (Wien)* 115:143–148
26. Kier EL, Staib LH, Davis LM et al (2004) MR imaging of the temporal stem: anatomic dissection tractography of the uncinate fasciculus, inferior occipitofrontal fasciculus, and Meyer's loop of the optic radiation. *AJNR Am J Neuroradiol* 25:677–691
27. Catani M, Howard RJ, Pajevic S et al (2002) Virtual in vivo interactive dissection of white matter fasciculi in the human brain. *Neuroimage* 17(1):77–94
28. Gaffan D, Easton A, Parker A (2002) Interaction of inferior temporal cortex with frontal cortex and basal forebrain: double dissociation in strategy implementation and associative learning. *J Neurosci* 22(16):7288–7296
29. Levine B, Black SE, Cabeza R et al (1998) Episodic memory and the self in a case of isolated retrograde amnesia. *Brain* 121(10):1951–1973
30. McKhann G, Drachman D, Folstein M et al (1984) Clinical diagnosis of Alzheimer's disease: report of the NINCDS-ADRDA Work Group under the auspices of Department of Health and Human Services Task Force on Alzheimer's Disease. *Neurology* 34(7):939–944
31. Fazekas F, Chawluk JB, Alavi A et al (1987) MR signal abnormalities at 1.5 T in Alzheimer's dementia and normal aging. *AJR Am J Roentgenol* 149(2):351–356
32. Masutani Y, Aoki S, Abe O, Hayashi N et al (2003) MR diffusion tensor imaging: recent advance and new techniques for diffusion tensor visualization. *Eur J Radiol* 46(1):53–66
33. Pajevic S, Pierpaoli C (1999) Color schemes to represent the orientation of anisotropic tissues from diffusion tensor data: application to white matter fiber tract mapping in the human brain. *Magn Reson Med* 42:526–540. Erratum in: *Magn Reson Med* 2000; 43(6):921
34. Makris N, Worth AJ, Sorensen AG et al (1997) Morphometry of in vivo human white matter association pathways with diffusion-weighted magnetic resonance imaging. *Ann Neurol* 42(6):951–962
35. Kunitatsu A, Aoki S, Masutani Y et al (2003) Three-dimensional white matter tractography by diffusion tensor imaging in ischaemic stroke involving the corticospinal tract. *Neuroradiology* 45(8):532–535
36. Lohmann G (1998) *Volumetric image analysis*. Wiley-Teubner, Chichester, pp 96–99
37. Kantarci K, Jack CR Jr, Xu YC et al (2001) Mild cognitive impairment and Alzheimer disease: regional diffusivity of water. *Radiology* 219(1):101–107
38. Schneider RC, Crosby EC, Bacchi BK et al (1961) Temporal or occipital hallucinations triggered from frontal lobe lesions. *Neurology* 11:172–179
39. Schneider RC, Crosby EC, Farhat SM (1965) Extratemporal lesions triggering the temporal-lobe syndrome. *J Neurosurg* 22:246–253
40. Schneider RC, Crosby EC, Calhoun HD (1982) Surgery of convulsive seizures and allied disorders. In: Schneider RC, Kahn EA, Crosby EC, Taren JA (eds) *Correlative neurosurgery*, vol. 1. Thomas, Springfield, pp 576–580